Entropy Driven Reversible Agglomeration of Crown Ether Capped Gold Nanoparticles

Alexander P. Hill[a], Casper Kunstmann-Olsen, Marcin P. Grzelczak and Mathias Brust*

Gold nanoparticles (AuNPs) continue to attract much attention across a broad range of research fields chiefly due to their optical properties[1], biocompatibility[2] and catalytic activity[3, 4]. Interparticle plasmon coupling resulting from the agglomeration of AuNPs can readily be exploited to create simple colorimetric test formats for analytical or diagnostic purposes[5-7]. In particular, the body of work by Mirkin and colleagues[8, 9] on the use of plasmon coupling in AuNPs for DNA and RNA analysis stands out as a significant ongoing development with many scientific and commercial ramifications. In recent years, a plethora of chemical and physical stimuli that can trigger the agglomeration of AuNPs have been identified including light[10], pH[11, 12], metal ions[13-15] and temperature[16, 17].

Nanoparticles that assemble upon cooling have been developed by functionalising with polymers that have upper critical solution temperatures (UCSTs), such as poly(N-acrlyoylglycinamide)[18] and poly(N,N'-dimethyl-(methacrylamido propyl) ammonium propanesulfonate)[19]. On the other hand nanoparticles that assemble upon heating are typically functionalised with polymers with lower critical solution temperatures (LCSTs), such as poly(N-isopropylacryamide), better known as pNIPAm[20], and oligo(ethylene glycol) terminated polymers such as poly(ethylene oxide-st-propylene oxide)[21]. Nanoparticles with thermo-responsive behaviour can prove useful to a wide range of applications such as cellular internalisation[22], controlled drug release[23], catalysis[24] and colorimetric sensors[25]. pNIPAm, one of the best-known thermo-responsive LCST polymers, has a phase transition that occurs at 31-32°C[26]. It has been observed that during this process pNIPAm forms coils within aqueous media followed by their collapse in order to form large insoluble globular structures, resulting in precipitation. A similar property has been seen in both PEG AuNPs[27] when at suitably high temperatures/ionic concentrations and oligo ethylene glycol (OEG) AuNPs when presented with suitable alkyl terminating groups[28].The agglomeration of functionalised nanoparticles at elevated temperatures is somewhat counterintuitive but typical for entropy driven processes such as hydrophobic interactions.

Crown ethers[29], cyclic oligomers of ethylene oxide, are known for their ability to strongly bind to specific cations, whilst being completely inert to others. This unique property is due to the hole-size cation-diameter relationship[30] and has resulted in their use for a variety of applications such as sensing[31, 32],phase transfer catalysis[33-35] and ion encapsulation[36]. With particular note given to Kotov[7] *et al* who developed long chain 18-Crown-6 capped GNps capable of detecting melamine via a similar agglomeration effect as described here.

We have recently shown that the use of thiolated crown ethers (18-C-6-CH_2-SH) as capping agents for gold nanoparticles allowed us to control the hydrophilicity via complexation of K^+ cations to the crown ether, resulting in phase transfer between aqueous and organic solvents[37]. Here we demonstrate that this ligand can also be used to prepare thermal-responsive particles that shows entropy driven reversible agglomeration with controllable transition temperatures directly related to the degree of cation complexation of the crown ether moiety (Scheme 1).

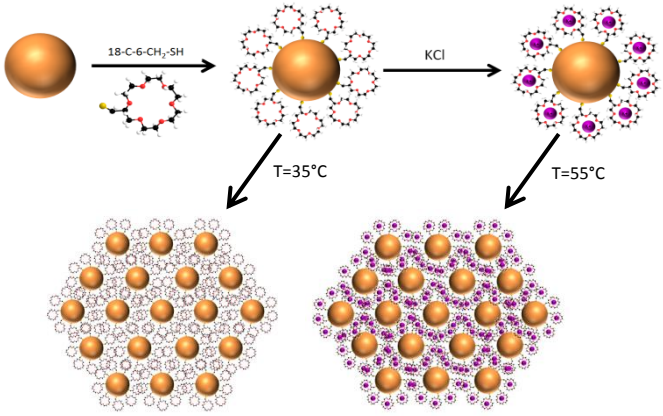

Scheme 1: *Illustration showing how the LCST of crown ether coated gold nanoparticles changes depending on the concentration/type of salt added to the local environment.*

Monodisperse gold nanoparticles with a diameter of 7-7.5nm were prepared using a modified citrate reduction method with the addition of tannic acid[38], resulting in particles with high stability in aqueous media. The particles were coated with thiolated crown ether (18-C-6-CH_2-SH) followed by the removal of excess ligand and salts *via* a two-step centrifugation process (14,600 rpm, 60min, 3°C and 13,000 rpm, 60min, 3°C). Reduced amounts of capping agent resulted in the slow aggregation of the particles whilst a large excess resulted in adhering, and therefore loss, of the particles to the walls of the holding containers during cleaning. Stable dispersions that did not adhere to surface were obtained typically using a preparative excess of 1500 to 2000 ligands per nanoparticle

[a] A. P. Hill
Department of Chemistry
University of Liverpool
Liverpool, L69 3BX
E-mail: sgahill@liv.ac.uk

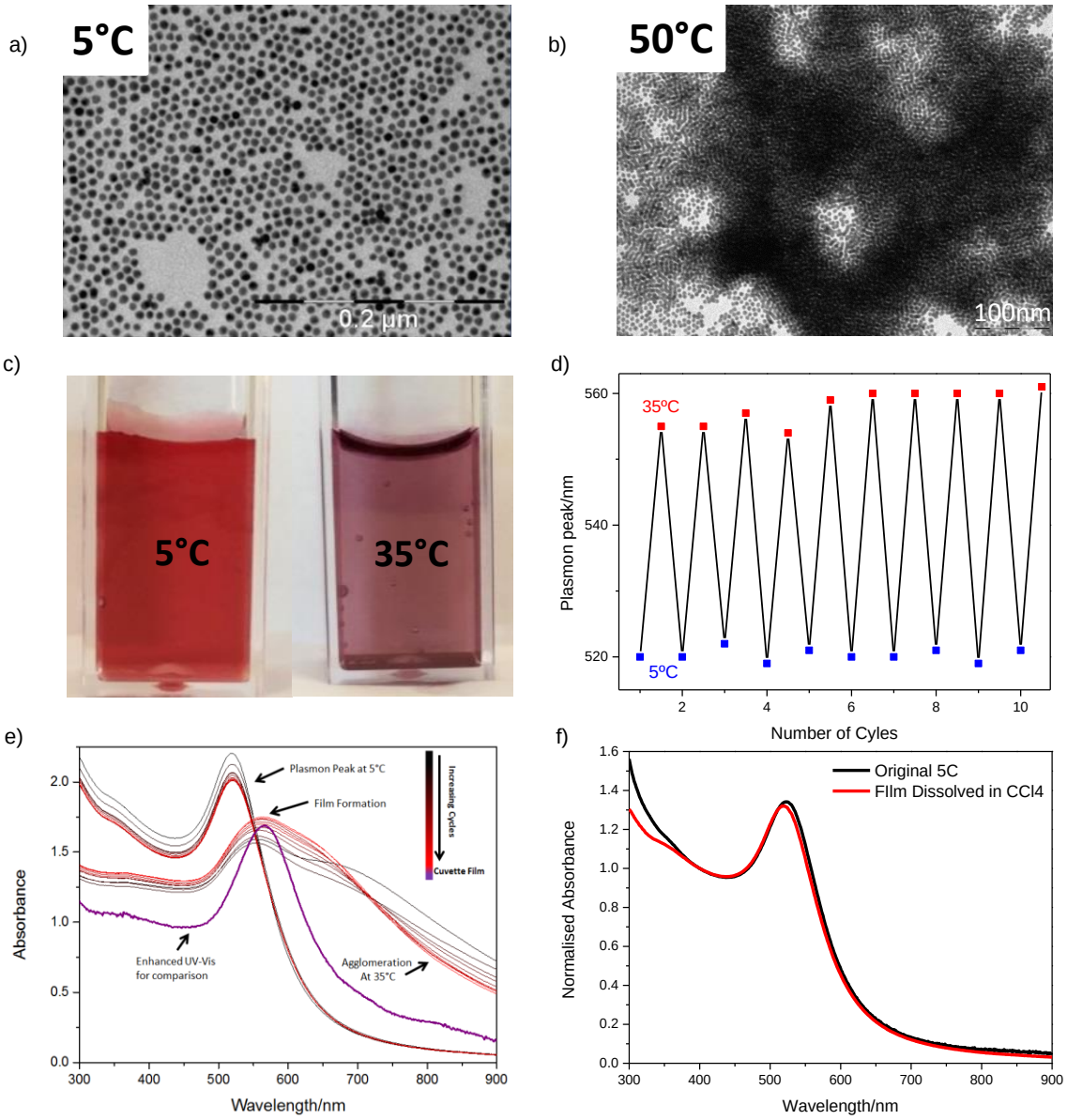

***Figure 1**: a) TEM grid immersed in a solution of 18-C-6-CH_2-SH coated AuNPs at 5°C , b) TEM grid coated in 18-C-6-CH_2-SH AuNPs at 50°C showing the extent of agglomeration at higher temperatures, c) change in colour upon repeated heating from 5-35°C, d) Peak maxima of the 5 and 35°C nanoparticles during temperature cycles , e) UV-Vis spectra showing the change in absorption throughout temperature cycles, including the cuvette film, f) UV-Vis spectra of cuvette film dissolved in chloroform compared to the original 5°C spectra.*

Aqueous dispersions of the 18-C-6-CH_2-SH AuNPs were subjected to a series of temperature cycles, alternating the temperature between 5° and 35°C. TEM images (figure 1a and 1b), were taken at two vastly different temperatures (5 and 50°C), to show in greater effect, the drastic change in particle behavior, from being highly stable as separate entities (5°C), to agglomerating into much larger structures (50°C), further TEM images can be seen within the *SI* which show the formation of these larger structures in greater detail. This process is apparent by the sudden colour change from red to purple that is observed upon heating above the agglomeration initiation temperature (30-31°C), as can be seen in figure 1c. Figure 1d shows the result of cycling the temperature repeatedly between 5 and 35°C. At each temperature extreme the peak position was measured and plotted to test for the reversibility of the agglomeration process. Over many cycles there appears to be no significant change in peak positions indicating that the particles returned to their original state after every cycle with a high degree of stability. The aggregation process is fully reversible.

In figure 1e the UV-Vis spectra taken at 5°C show a gradual small decrease in absorbance with each temperature cycle. The reverse trend is manifested in the UV-Vis spectra recorded at 35°C, with the plasmon peak at 555 nm increasing gradually with every cycle. This can be attributed to a slow film formation process, which begins at 35°C and is not reversible in aqueous media. The film itself has an absorbance maximum at 555 nm and hence contributes additively to the spectra at 35°C. It has very little absorbance at 520 nm and therefore the loss of material through film formation is manifested in a gradually decreasing peak absorbance at 5°C. This decrease is also observed far away from the peaks at 800 nm and above, another region where the film absorbs very little. Note the isosbestic point at 720 nm indicating that a single simple process is responsible for both the increase and the decrease of the absorbance at different wavelengths. The film contributes to the absorbance close to 555 nm and detracts from it at wavelengths where its absorbance is low. Further evidence for film formation was provided by removal of the AuNP solution and measurement of the empty cuvette (figure 1e). The plasmon peak of the film is at 560 nm and coincides well with that of the dispersion at 35°C. The film was dispersible in chloroform, and the optical spectrum of the resulting dispersion could be compared to the original 5°C spectra (figure 1f) The two spectra

align perfectly, with the shift in plasmon resonance being attributed to the change in the solvent refractive index[39] rather than any loss of stability[40].

As shown in figure 4 a, the agglomeration of the 18-C-6-CH_2-SH coated AuNPs in the absence of salt occurs at 30°C with a steep shift of the plasmon peak position and little change after reaching a plateau. Upon adding 1mM NaCl, the transition occurs within the same temperature range but with a slightly steeper rise whilst the addition of 1mM LiCl results in no change. Upon addition of 1mM KCl the transition temperature shifts dramatically from 30 to 42°C. This trend continues with increasing concentration of KCl. We attribute this specific dependence of the agglomeration temperature on the KCl concentration to the strong and specific complexation of potassium ions by the 18-C-6 crown ether ligand.

The zeta potential of each system was measured to determine whether the overall charge of the AuNPs in solution was indeed related to the changes in transition point (figure 2b). In the absence of salt, the AuNPs have a zeta potential of -8 mV. Upon the addition of 1mM LiCl this remains unchanged which results in the transition point of the system also remaining unchanged. The addition of 1mM NaCl results in a slightly more positive zeta potential (-2mV), a difference of +6mV, whilst the addition of 1mM KCl results in a significant shift of the zeta potential to +17.5mV. It can be seen from the data that even the addition of 0.25mM KCl results in a far greater change of net charge than either NaCl or LiCl. Relating the zeta potentials to the LCST transition temperatures makes it very clear that only ions that are strongly complexed by the crown ether significantly affect the LCST transition point.

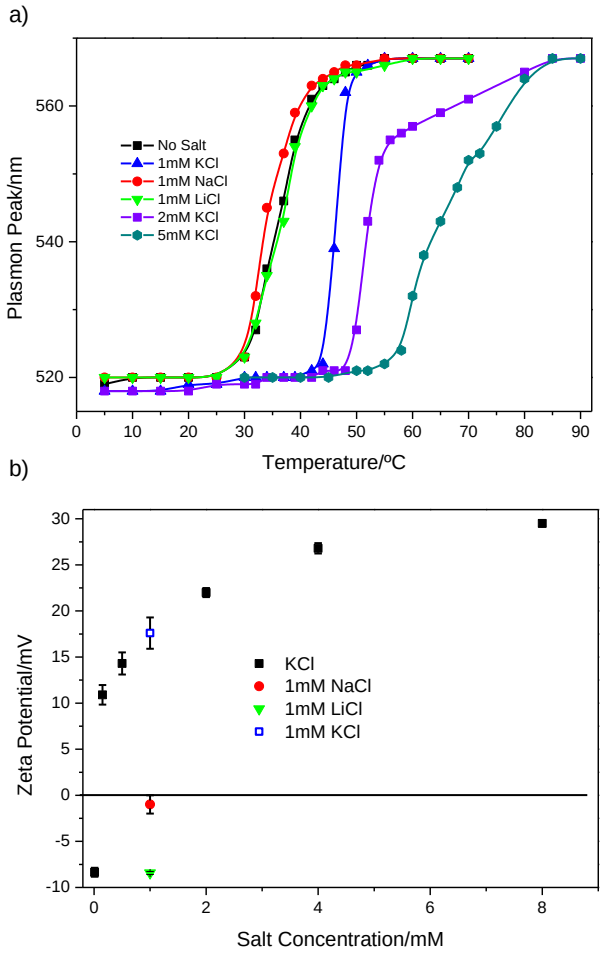

Figure 2: *a) Plasmon Peak position as a function of temperature at different salt concentrations b) Zeta potential as a function of potassium concentration and in the presence of 1 mM non-compolexing ions (NaCl and LiCl).*

Even in the absence of calorimetric data, which we have been unable to obtain so far, the relation between zeta potential and transition temperature can be illustrated qualitatively with help of the Gibbs Helmholtz equation.

$$\Delta G = \Delta H - T\Delta S$$

ΔG for the agglomeration process must be zero at the transition temperature and has a negative value at more elevated temperatures. This observation indicates an entropy driven process, *i.e.* ΔS is positive and is the energetic driving force of the process. This is typical for hydrophobic interactions and relates to the large number of confined water molecules that are freed up in this process. How do we explain the increase in transition temperature with increasing potassium concentration? This suggests an endothermic process, *i.e*. ΔH is positive and dependent of the degree of complexation of the crown ether moieties. The more positive charge is present the more energy will be needed to hold the agglomerates together. For this reason, with increasing complexation, ΔH will also increase, and so does the temperature at which this increase is compensated by the entropy term. This explains the temperature dependence of the transition point. In the absence of complexed cations, after careful cleaning of the colloid by repeated centrifugation, aggregation no longer takes place. This is due to the increased hydrophilicity of the un-complexed crown ether moiety which no longer provides an entropic driving force for aggregation.

In order to monitor the agglomeration process of these particles in more detail, their apparent size change with increasing temperature was monitored using dynamic light scattering (DLS) (Figure 3a). At 5°C the particles are stable and correctly sized at 7nm. As the temperature increased and reached the transition point the DLS showed a mixture of two particulate sizes, 7nm particles as well as much larger 150nm particulates. Upon increasing the temperature further, up to 40°C, the DLS showed only one size of particulate at 1000nm in size, further increases in temperature did not result in any further changes in size. The appearance of two distinct peaks in the DLS spectra is typical for anisotropic shapes of particles or agglomerates. For example, it is also observed for gold nanorods[41] Here we interpret this as initial linear assembly of particles, which is often the case in destabilising charged colloidal systems[42]. Indeed, a careful revision of figure 1e reveals in one of the spectra of aggregated particles a hump at 700 nm. This spectrum must have been taken at a slightly earlier stage of agglomeration and is also indicative of initial linear assembly with the appearance of an embryonic longitudinal plasmon band[43].

The TEM image (figure 3b) sampled during aggregation also shows extended linear structures that could have formed already in the dispersed phase. Current work in our laboratory on the agglomeration and film formation processes aims to exploit these findings for the creation of structurally and functionally interesting new materials.

a)

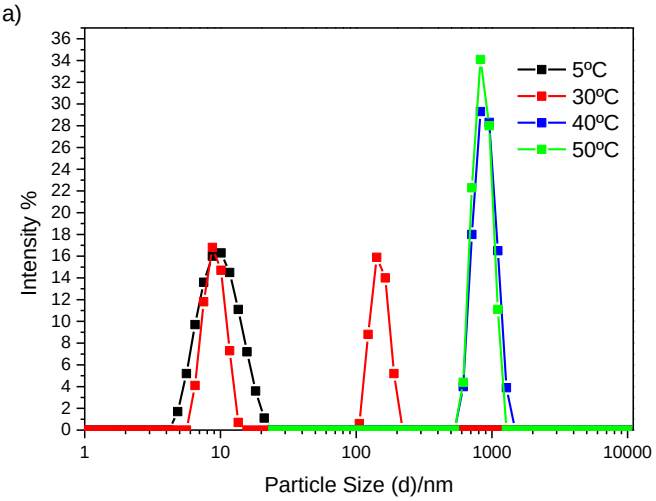

b)

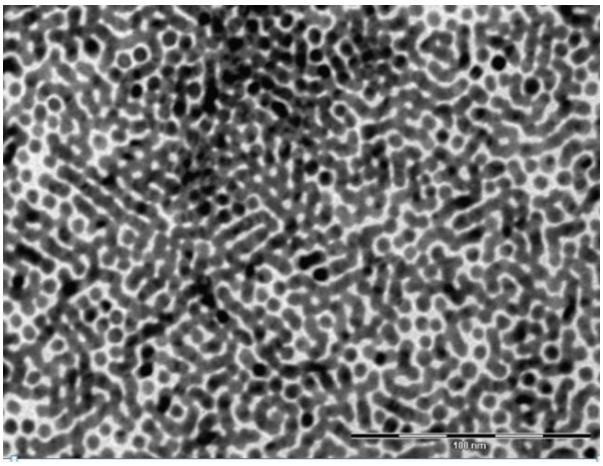

Figure 3: *a) DLS showing the change in particulate size and shape with increasing temperature, b) TEM of the agglomerate formation of 18-C-6-CH_2-SH AuNPs sampled after phase transition.*

In conclusion, based on a typical gold colloid and the small functional thiolated ligand, 18-C-6 crown ether, we have developed a thermo-responsive AuNP system that shows fully reversible entropy driven agglomeration at elevated temperatures. Uniquely, the transition temperature can be finely tuned over a significant range by specific complexation of the ligand with potassium ions. Film formation and anisotropic aggregation are under investigation. Materials like the one described here may have future uses as sensors, actuators electronic components, thin film ion batteries and ion selective electrodes.

1. K. A. Willets and R. P. Van Duyne, *Annu. Rev. Phys. Chem.*, 2007, **58**, 267-297.
2. L. A. Dykman and N. G. Khlebtsov, *Chemical reviews*, 2013, **114**, 1258-1288.
3. M. Stratakis and H. Garcia, *Chemical Reviews*, 2012, **112**, 4469-4506.
4. M.-C. Daniel and D. Astruc, *Chemical reviews*, 2004, **104**, 293-346.
5. K. Saha, S. S. Agasti, C. Kim, X. Li and V. M. Rotello, *Chemical reviews*, 2012, **112**, 2739-2779.
6. S.-Y. Lin, S.-W. Liu, C.-M. Lin and C.-h. Chen, *Analytical Chemistry*, 2002, **74**, 330-335.
7. H. Kuang, W. Chen, W. Yan, L. Xu, Y. Zhu, L. Liu, H. Chu, C. Peng, L. Wang, N. A. Kotov and C. Xu, *Biosensors and Bioelectronics*, 2011, **26**, 2032-2037.
8. R. Elghanian, J. J. Storhoff, R. C. Mucic, R. L. Letsinger and C. A. Mirkin, *Science*, 1997, **277**, 1078-1081.
9. C. A. Mirkin, R. L. Letsinger, R. C. Mucic and J. J. Storhoff, *Nature*, 1996, **382**, 607-609.
10. R. Klajn, K. J. Bishop and B. A. Grzybowski, *Proceedings of the National Academy of Sciences*, 2007, **104**, 10305-10309.
11. C. J. Orendorff, P. L. Hankins and C. J. Murphy, *Langmuir*, 2005, **21**, 2022-2026.
12. J. Song, J. Zhou and H. Duan, *Journal of the American Chemical Society*, 2012, **134**, 13458-13469.
13. Y. Kim, R. C. Johnson and J. T. Hupp, *Nano Letters*, 2001, **1**, 165-167.
14. H. N. Kim, W. X. Ren, J. S. Kim and J. Yoon, *Chemical Society Reviews*, 2012, **41**, 3210-3244.
15. J. S. Lee, M. S. Han and C. A. Mirkin, *Angewandte Chemie*, 2007, **119**, 4171-4174.
16. A. Housni and Y. Zhao, *Langmuir*, 2010, **26**, 12933-12939.
17. Y. Liu, X. Han, L. He and Y. Yin, *Angewandte Chemie International Edition*, 2012, **51**, 6373-6377.
18. F. Liu and S. Agarwal, *Macromolecular Chemistry and Physics*, 2015, **216**, 460-465.
19. C. Durand-Gasselin, R. Koerin, J. Rieger, N. Lequeux and N. Sanson, *Journal of colloid and interface science*, 2014, **434**, 188-194.
20. S. Chakraborty, S. W. Bishnoi and V. c. H. Pérez-Luna, *The Journal of Physical Chemistry C*, 2010, **114**, 5947-5955.
21. C. Durand-Gasselin, M. Capelot, N. Sanson and N. Lequeux, *Langmuir*, 2010, **26**, 12321-12329.
22. S. Salmaso, P. Caliceti, V. Amendola, M. Meneghetti, J. P. Magnusson, G. Pasparakis and C. Alexander, *Journal of Materials Chemistry*, 2009, **19**, 1608-1615.

23. M. Pernia Leal, A. Torti, A. Riedinger, R. La Fleur, D. Petti, R. Cingolani, R. Bertacco and T. Pellegrino, *ACS nano*, 2012, **6**, 10535-10545.
24. X.-Y. Liu, F. Cheng, Y. Liu, H.-J. Liu and Y. Chen, *Journal of Materials Chemistry*, 2010, **20**, 360-368.
25. X.-Y. Liu, F. Cheng, Y. Liu, W.-G. Li, Y. Chen, H. Pan and H.-J. Liu, *Journal of Materials Chemistry*, 2010, **20**, 278-284.
26. D. Roy, W. L. Brooks and B. S. Sumerlin, *Chemical Society Reviews*, 2013, **42**, 7214-7243.
27. D. n. Zámbó, G. r. Z. Radnóczi and A. s. Deák, *Langmuir*, 2015, **31**, 2662-2668.
28. R. Iida, H. Mitomo, Y. Matsuo, K. Niikura and K. Ijiro, *The Journal of Physical Chemistry C*, 2016, **120**, 15846-15854.
29. C. J. Pedersen, *Angewandte Chemie International Edition*, 1988, **27**, 1021-1027.
30. G. W. Gokel, D. M. Goli, C. Minganti and L. Echegoyen, *Journal of the American Chemical Society*, 1983, **105**, 6786-6788.
31. G. W. Gokel, W. M. Leevy and M. E. Weber, *Chemical reviews*, 2004, **104**, 2723-2750.
32. J. Li, D. Yim, W.-D. Jang and J. Yoon, *Chemical Society Reviews*, 2017, **46**, 2437-2458.
33. M. E. Childs and W. P. Weber, *The Journal of Organic Chemistry*, 1976, **41**, 3486-3487.
34. D. Landini, F. Montanari and F. M. Pirisi, *Journal of the Chemical Society, Chemical Communications*, 1974, 879-880.
35. A. E. Visser, R. P. Swatloski, W. M. Reichert, S. T. Griffin and R. D. Rogers, *Industrial & Engineering Chemistry Research*, 2000, **39**, 3596-3604.
36. F. Lucio-Martínez, B. Bermúdez, J. M. Ortigueira, H. Adams, A. Fernández, M. T. Pereira and J. M. Vila, *Chemistry-A European Journal*, 2017, **23**, 6255-6258.
37. M. P. Grzelczak, A. P. Hill, D. Belic, D. F. Bradley, C. Kunstmann-Olsen and M. Brust, *Faraday Discussions*, 2016, **191**, 495-510.
38. J. Piella, N. G. Bastús and V. Puntes, *Chemistry of Materials*, 2016, **28**, 1066-1075.
39. P. Mulvaney, *Langmuir*, 1996, **12**, 788-800.
40. G. C. Papavassiliou, *Progress in Solid State Chemistry*, 1979, **12**, 185-271.
41. X. Liu, Q. Dai, L. Austin, J. Coutts, G. Knowles, J. Zou, H. Chen and Q. Huo, *Journal of the American Chemical Society*, 2008, **130**, 2780-2782.
42. S. Glotzer, M. Solomon and N. A. Kotov, *AIChE Journal*, 2004, **50**, 2978-2985.
43. I. Hussain, M. Brust, J. Barauskas and A. I. Cooper, *Langmuir*, 2009, **25**, 1934-1939.